Research Article

Assessment of On-going tectonic deformation in the Goriganga River Basin, Eastern Kumaon Himalaya Using Geospatial Technology

M Nazish Khan*
Center of Applied Remote Sensing and GIS Technology, Samarkand State University, Samarkand, Uzbekistan

Himanshu Govil
Department of Applied Geology, National Institute of Technology, Raipur (Chhattisgarh), India

*Corresponding author. E-mail: nazishgeo@gmail.com

How to Cite

Khan M. N. and Govil H. (2023). Assessment of On-going tectonic deformation in the Goriganga River Basin, Eastern Kumaon Himalaya Using Geospatial Technology. *Journal of Applied and Natural Science*, 15(4), 1679 - 1690. https://doi.org/10.31018/jans.v15i4.5068

Abstract

The Goriganga river basin lies in the Northeast Kumaon Himalaya and is found suitable for assessing active tectonics at different scales. In addition, this study focuses on the assessment of ongoing tectonic activity through morphotectonic measurement of the Goriganga river basin, which is an ideal location for such analysis and Goriganga river basin transects with three major domains of Himalaya's lithotectonic structures viz., Tethys, Vaikrita, and Lesser Himalayan Domain. To realize this task, the ASTER Digital Elevation Model was used and found suitable to extract different morphotectonic indices such as Stream Length Gradient (SL), Hypsometric Integral (HI), Length of Overland Flow (Lg), Drainage Density (Dd) and Channel Sinuosity (Cs). Results of these important indices, including SL (18- 4737) HI (0.26- 0.57), and Lg (0.08- 0.19) depict greater variability in the tectonics activity while these values are correspondingly high in the close proximity of lithotectonic units, showing strong tectonic activity. In the extreme south, the Rauntis Gad basin strongly influences tectonism due to transecting syncline and anticline as well as unknown active faults.

Keywords: Active Tectonics, ASTER, Digital Elevation Model, Morphotectonics

INTRODUCTION

The tectonic and surface processes work in tandem to carve landscapes and landforms, which indeed bear an imprint of these processes' relative timing and magnitude. The repercussions of tectonic uplift on surface processes, viz., weathering and erosion, have long been conceded, while the effects of weathering and erosion on tectonics, have invoked attention only in recent years (Willett et al., 2006; Farooq et. al., 2015; Khan et. al., 2023). Active tectonics is significantly helpful in assessing and analyzing the deformation of the earth's crust on a time scale, significant to human society (Keller and Pinter, 2002; Omar and Mosar, 2019). Active tectonics establishes a critical relationship between tectonics and geomorphological processes that shape the earth's surface (Burbank and Anderson, 2011; Taib et. al., 2023). Further, the impact of such processes is measured by computing geometry, topography, and shape of the earth's surface and the temporal change thereof (Turner, 2006). It was deciphered from basin morphometric indices, which are crucial to record the presence of faults, thrusts, and shear zones, active ruptures, displaced landforms, and influence on landform evolution (Wallace, 1990). The presence of active faulting on landscapes may be displayed by the offset of river channels, forming lakes, and developing meanders (Tricart, 1974). Further, the effects of active faulting across a river can be manifested in the form of alignment of drainage patterns along faulting and sometimes irregular (Twidale, 1971). In tectonically active regions, drainage is used as a proxy to cognize evolution of landscape (Goldsworthy and Jackson, 2000). It is evident that Himalayan region is tectonically active and its geomorphic setting and behavior are controlled by the tectonic quiescence between uplift and erosion along major and minor rivers (Joshi and Kotlia; 2015, Kotlia et al., 2010, Kothyari et

al., 2017, Valdiya 1976, 1992, 2000). Many workers have postulated that the geomorphic evolution of Himalayan Thrust Belts is operated under the control of external factors including tectonic uplift, weathering, and erosion etc. (Bookhagen and Burbank, 2006: Joshi and Kotilia, 2015; PérezPena, Azor, Azanón, and Keller, 2010; Pazzaglia, 2013; Kothyari et al., 2008; Valdiya, 1993). The Goriganga River basin lies across Trans Himadri Fault (THF), Main Central Thrust (MCT), Berinag Thrust (BT), North Almora Thrust (Pathak, Pant and Dharmwal, 2013; Valdiya, 1976, 2003), and transecting with many unknown faults i.e., Rauntis Fault. Therefore, it is particularly an ideal site for the quantification of geomorphic features which evolved due to tectonic activity, which lies in the recognized faults and thrusts. Geomorphic signs concomitant with faults and thrusts in the region are incised meanders, formation of lakes/ paleolakes, offset of rivers, landslides, strath terraces and vertical gorges etc. (Mohammad, 2014; Farooq et al., 2015; Farooq and Khan, 2017; Pathak et al., 2013; Bookhagen et al., 2013; Kothyari et al., 2020) and impact of land use and land cover on neo-tectonic activity (Khan et al., 2023). This study aimed to highlight the neo-tectonics deformation in the eastern Kumaun Himalaya where the Goriganga river basin is the suitable site for the assessment.

MATERIALS AND METHODS

Study area

The Goriganga River starts its journey from Milam Glacier, located south of the Nanda Devi Peak in Tethys Himalaya. This basin lies between latitudes 29° 45'03" to 30°35'53" north and longitudes 79°59'10" to 80°29'25" east and is elongated in the NNW-SSE direction. It covers a 99.2 km distance before confluence with Kali River at Jauljibi with a catchment area of 2242.4 km^2.

Glaciers dominate the northern extremity of the Goriganga river basin and covers 605 km2 (27%) area under dense ice cover. The Dhauliganga River shares its boundary in the northeast and the Ramganga River in the southwest and it flows southwards for a considerable distance. Geologically, the Goriganga River basin transects with three domains of Himalaya viz., the northeastern part of the basin (415.68 km2) lies over the Tethys domain, the Central or northwestern part (1228.46 km2) over the Higher Himalaya, separated by THF in the north and MCT in the south and southern part (599.76 km2) lies over the Lesser Himalaya (Fig.1). Therefore, the Gorigranga River basin is found suitable for morphotectonic assessment.

Geologic Setting

The Goriganga River basin comprises three major domains of tectonics with an extent of 99.2 km from north to south. The geological formations of the Tethys domain are represented by a thick late Proterozoic to late Cretaceous sedimentary cover, termed Tethys sediments, lying over the crystalline basement, which represents the distal continental margin of the Indian shield.

The Higher Himalayan Crystallines (HHC) dominate the Central part of the basin, which includes high-grade metamorphic
rocks of Precambrian, Paleozoic, and Early Mesozoic ages (Metamorphic rocks) which metamorphosed during the late Eocene to early Miocene and invaded by granites of Miocene age (Larson and Godin, 2009, Valdiya, 2001).

After crossing the Main Central Thrust (MCT) or Munisiari Thrust (MT), the river flows through the Almora Group of rocks and Mandhali Formation near Munisiari (Valdiya, 1980). Further, it flows through Rautgarh and Gangolihat Formations and transects with numerous transverse faults as the Baram fault before the confluence with Kali River (Fig. 2). Lithotectonic units, faults, and thrusts indicate that the Goriganga River follow different litho-structural features from Trans Himadri Fault to many transverse faults up to the outlet.

Drainage Pattern

Gorigana is a monsoon and glacier-nursed river that originates at more than 5000 meters above the mean sea level from Milam Glacier in the south of Nanda Devi Peak. It runs through glaciated broad floored, U-
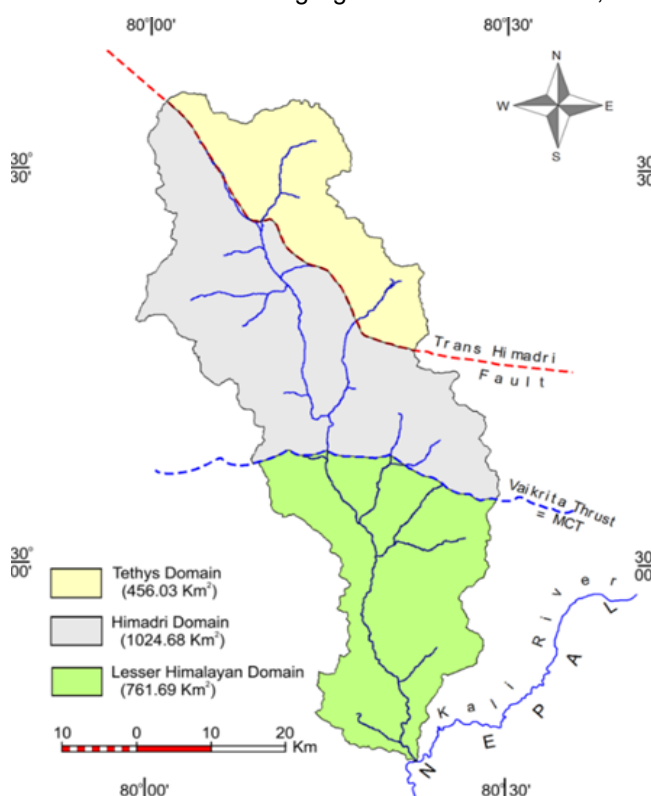

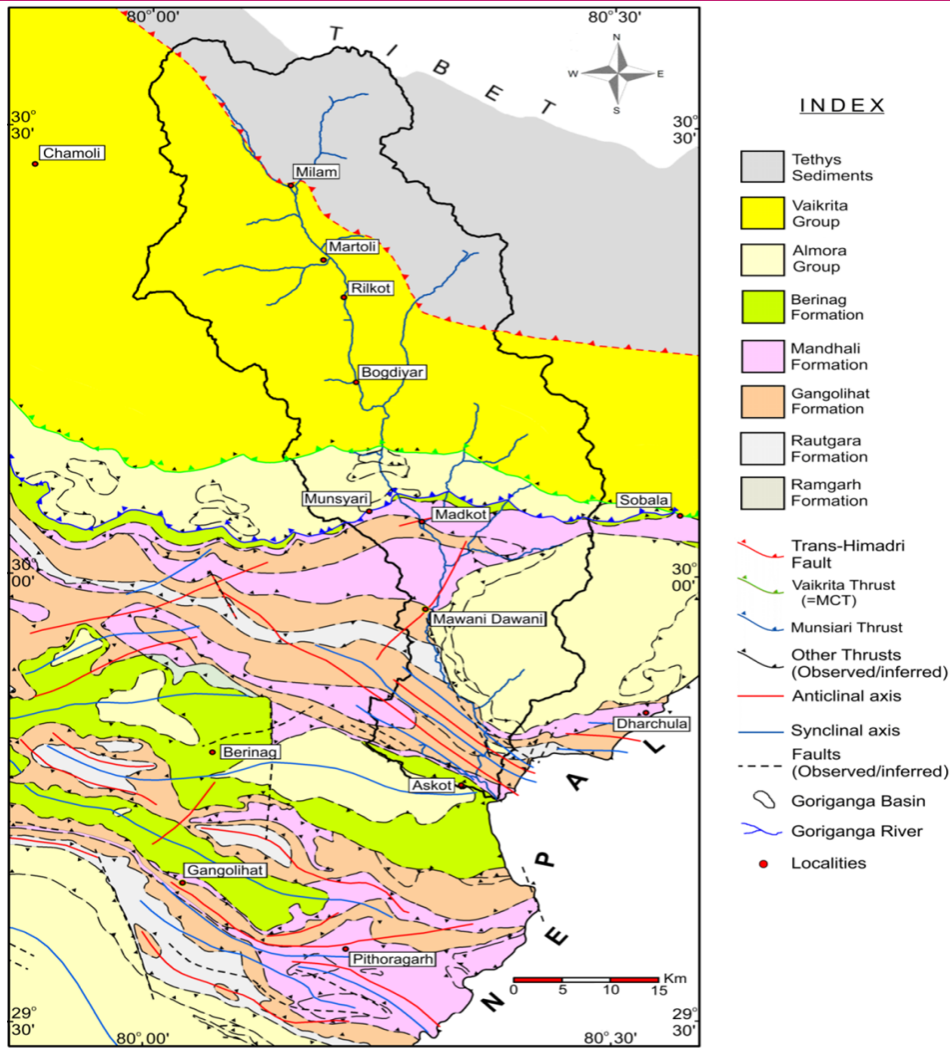**Fig. 1.** *Showing the study area along with major litho-tectonic domain*

Fig. 2. *Geological map of the study area, transects with Trans Himadri Fault, Vaikrita Thrust and Munisiari Thrust (Modified after Valdiya (2008) and Sharma and Paul (1988)*

shaped valleys up to a considerable distance. Broad floored valleys turn into deep V-shaped canyons as it enters the Thrust Zone. Goriganga River takes nearly a right-angle turn when it crosses the Trans Himadri Fault, where Paleolake was studied by Valdiya (2001), Kotlia and Rawat (2004) and Kotlia and Joshi (2013). It creates an S-shaped meander near Bogdyar before crossing Main Central Thrust and many river offsets and strath terraces have been perceived downside when it passes the Baram Fault near Toli village.

Climatologically, the Goriganga river basin comprises considerable diversity from south to north, influencing the topographic evolution of monsoon and glacially fed regions of Kumaon Himalaya, creating distinct morphotectonic zones.

In the southern portion of the river basin, monsoon produces torrential rainfall that modifies or carves the landscape and drainage pattern, while the northern part comprises a glacial climate which creates broad floored valleys and sharp ridges which are tectonically active in the presence of well-known Trans Himadri Fault (THF).

Data analyses

In the present work, morphotectonic analyses were based on integrating several datasets acquired through remote sensing, GIS, and fieldwork. Advanced spaceborne Thermal Emission and Reflection Radiometer (ASTER) data derived Digital Elevation Model (DEM) was obtained from USGS Earth Explorer and input into the GIS environment for further analysis. The Aster Instrument was built to collect orthoimages for deriving digital elevation models by Japan's Ministry of Economy, Trade and Industry (METI) and the National Aeronautical and Space Administration (NASA). It was launched in December 1999 and acquired data in 14 bands using three different telescopes and sensor systems. Images were acquired in three visible and near-infrared bands with a spatial resolution of 15 m, six short-wave-infrared bands with a spatial resolution of 30 m, and five thermal infrared (TIR) bands that have a spatial resolution of 90 m (ASTER Validation Team, 2009). Further, ASER digital elevation model with 30-meter resolution was generated using level-1A scenes

Table 1. ASTER GDEM characteristics (ERSDAC, 2011)

Tile Size	3601 x 3601 pixels (1° X 1°)
Posting Interval	1 arc-second
Geographic coordinates	Geographic latitude and longitude (GCS)
DEM output format	GeoTIFF signed 16 bits, and 1 m/DN Referenced to the WGS84/EGM96 geoid
Special DN values	-9999 for void pixels, and 0 for seawater body
Coverage	North 83° to south 83°, 22,600 tiles for Version 1
Abnormality Removal	By stacking cloud-masked and non-cloud-masked scenes

(Table 1).

Topographic maps at a scale of 1:250000 scale were acquired from Army Map Services, which publishes it on behalf of the University of Texas at Austin, which is responsible for the publication and distribution of these maps. The downloaded maps were georeferenced to UTM projection and WGS84 datum using Global Mapper 13. These georeferenced maps were used for vectorizing the locations of villages and small towns/ cities in the Goriganga river basin. It also provided additional GIS input to compare the accuracies of drainage networks and watershed boundaries.

Geological information about lithology, significant tectonic features such as thrusts and dislocations, and smaller faults, joints, and shear zones, was primarily collected from Valdiya (2010) revised geological map of the Kumaon Himalaya. To be consistent with the ASTER DEM and multispectral data used in this work, the map was georeferenced to the UTM projection and WGS84 datum. Additionally, published geological maps of the Kumaon Himalaya that had a geographic referencing coordinate system and could thus be georeferenced were used to collect geological data (Fig. 2).

Watershed boundaries and detailed drainage networks were extracted using ArcGIS and TauDEM plugins due to their reproducible and accurate results. However, the conventional digitization method was avoided due to its time-consuming and non-reproducible nature. The automated watershed and drainage network extraction method is the most favored and widespread for studying watersheds.

Stream networks and basin boundaries derived by the TauDEM (Terrain Analysis Using Digital Elevation Models) plugin and further various hydrologic characteristics formulated using digital elevation data of the study area. These hydrologic grids are put into the GIS domain to locate all sites within the DEM upstream of the designated outlet point to define the borders (Farooq et al., 2015). The watershed delineation process involves four main steps: filling in 'pits' in the raw DEM, figuring out the flow direction from each grid cell, figuring out the flow accumulation, stream grids, and drainage area for each cell, and drawing the boundaries of the watershed by working backward from the flow direction grid. To provide comprehensive coverage of the Goriganga river basin, four ASTER DEMS scenes

(ASTGTM_N290E079, ASTGTM_N29E080, ASTGTM_N30E079, and ASTGTM_N30E080) were tiled. The following was the data processing process for stream network and watershed delineation:

The Digital Elevation Model (DEM) typically comprises low-elevation sections that were bordered by higher topography that impedes a smooth flow. Low-elevation sections might not always be found naturally; they might occasionally be straightforward artifacts created during continuous slope modeling. Low elevation section filling is done by merely increasing the elevation of a cell designated as a pit until it is equal to the elevation of its uphill neighbor.

The pit-filled DEM was used to calculate the flow direction from each grid cell to its next downhill neighbor. The pit-filled data (hydrologically corrected) is given as input for deriving the slope of each grid cell, named the D8 flow direction. The output numerically encodes the steepest descent direction from each grid as 1 = East, 2 = North East, 3 = North, 4 = North West, 5 = West, 6 = South West, 7 = South and 8 = South East.

This step involves of delineating flow accumulation, stream grids, and drainage areas. The total number of uphill cells that flow to any given cell was determined using the flow direction grid. During this step, a summing was done for all cells within a dataset to create a flow-accumulation grid. It is based on a total number of upslope cells flowing into a downslope-flowing cell.

In last, so far generated hydrologic grids input for delineating watershed boundaries. For this purpose, an outlet was specified at the confluence of Goriganga with Kaliganga River and boundaries were derived through the specified outlet. Further, these layers are converted to a polygon, representing the boundaries. Using ArcMap 10.7, the Goriganga catchment was distributed into 32 watersheds for detailed drainage network and watershed analysis by entering an optimum threshold during delineation. Further, a detailed drainage network was derived from Aster Digital Elevation Model (DEM) and used to extract and calculate the following morphotectonic indices for assessment and mapping variation in tectonic activity considering lithotectonic features (Table 2).

Stream Length Gradient
Through differential erosion, rivers sculpt the surround-

Table 2. Indices used for the computation of morphotectonic parameters

Aspects	Morphometric parameters	Formula	Reference
Linear	Channel Sinuosity (C_s)	$C_s = S_l/V_l$, where S_l = Stream length, V_l = Valley length	Mueller (1968)
Aerial	Drainage Density (D_d)	$D_d = L_u/A$, where L_u = Total stream length of all orders, A = Area of basin (km^2)	Horton (1932)
	Length of Overland Flow (L_g)	$L_g = 1/D_d \times 2$, where D_d = Drainage Density	Horton (1945)
	Hypsometric Integral (HI)	HI = $(EL_{mean} - EL_{min}) / (EL_{max} - EL_{min})$ where EL_{mean} is the mean elevation, EL_{min} is the minimum and EL_{max} the maximum elevation	Strahler (1952)
Relief	Valley Floor Width to Height Ratio (V_f)	$V_f = 2V_{fw}/ (E_{ld}-E_{sc}) + (E_{rd}-E_{sc})$, where V_{fw} = width of valley floor, E_{ld} and E_{rd} = Elevation of left and right valley divides, E_{sc} = Elevation of the valley floor	Bull and McFadden (1977)
	Stream-length gradient index (SL)	SL = $\Delta h /\Delta l \times L$, where Δh = Difference in elevation of the ends of the reach, Δl = Length of reach, L = distance from the midpoint of reach to the most distant point upstream	Hack (1973)

ing rocks and soils at varying rates, changing the landscape (Hack, 1973). As the rate of uplift is balanced by the rate of erosion and the river system has a slightly concave longitudinal profile (Schumm et al., 2002), the processes of erosion and uplift indicate crustal stability. Tectonic, lithological and climatic variables deviate from this dynamic equilibrium (Hack, 1973). Hack (1973) proposed an indicator termed the Stream Length Gradient Index to assess gradient in river systems. It is defined as

$$SL= \left(\frac{\Delta H}{\Delta L}\right) \qquad (1)$$

Where SL is the stream-length gradient index, ΔH is the change in elevation of the channel reach under investigation, ΔL is the length of the reach and L is the total planimetric length from the midpoint of the reach to the highest point on the channel (Mahmood and Gloaguen, 2012). The SL index assesses relative tectonic activity (Keller and Pinter, 2002). High values of SL indicate recent tectonic activity while high values indicate low tectonic activity. However, anomalously low values may also be associated with tectonic activity when streams and rivers flow along strike-slip faults (Keller and Pinter, 2002).

Hypsometric Integral (HI)

The hypsometric integral is alluring for morphometric investigations since it is a dimensionless parameter and enables scale-independent comparison of various catchments. According to Strahler, low values indicate ancient, eroded landscapes in the final stages of geomorphic evolution, while high values indicate younger, less eroded landscapes where the uplift was outpacing surface denudation processes, meaning that a signifi-

cant portion of the basin's rock mass remains to be removed (Dowling et al., 1998). The volume of the basin above its lowest point, which has not been eroded, is expressed by the hypsometric integral.

The integral explains the distribution of elevation in a certain area of the terrain, particularly a drainage basin. It is defined as:

$$HI = \frac{(EL_{mean} - EL_{min})}{(EL_{max} - EL_{min})} \qquad (2)$$

Where EL_{mean} is the mean elevation, EL_{min} the minimum and EL_{max} is the maximum elevation within the drainage basin as extracted from a DEM.

The range of hypsometric values is 0 to 1. Due to the high processing involved, hypsometric analysis has not been used as much in the past. However, with the accessibility of digital elevation data and the advancements in computing and GIS technologies, hypsometry is a useful technique to measure watershed parameters objectively (Dowling et al., 1998).

Length of Overland Flow (Lg)

A network of flow paths downslope to the nearest canal via surface runoff follows the drainage divide. According to Horton (1945), the length of time that water travels over land before entering a particular stream route is known as the length of overland flow (Lg). The length of overland flow is estimated by:

$$L_g = \frac{1}{2D_d} \qquad (3)$$

where drainage density is denoted by Dd. The overland flow length is almost half the drainage density (Dd) and roughly half the average distance between stream channels. It thus provides a measure of drainage basin

efficacy. If the overland flow values are smaller, surface runoff will enter streams more quickly. It indicates the concentration or stream frequency of a region and is directly correlated with the infiltration rate. There are typically fewer streams per unit area in a river basin with permeable rocks than one with impermeable rocks. In fact, L_g is largely controlled and affected by the degree of slope, geological conditions of lithology and structure, soil characteristics, vegetation cover, rainfall intensity and infiltration capacity (Ghosh, 2011). L_g is basically inversely proportional to the average slope of the stream and is synonymous with the length of sheet flow. One important aspect of Lg, it does not directly exhibit the active tectonic status of a drainage basin, it can nevertheless serve as a proxy indicator of active tectonics, in that smaller values of L_g are indicative of steeper gradients and, therefore, of greater degree of tectonic turmoil.

Drainage Density (Dd)

Horton (1932) established drainage density (Dd) as a significant morphometric term. Dd is the ratio of the total channel length of streams of all orders in a basin to the basin area. Dd is a crucial sign of the linear scale of fluvial topographic landform components. It provides a numerical measurement of the typical length of the stream channel for the basin and illustrates how closely spaced the channels are. In places with highly permeable subsurface material under extensive vegetation cover and/or areas with low relief, a low drainage density is more likely to occur, according to measurements of drainage density done over a wide range of geologic and climatic types. High relief, limited vegetation, and weak or impermeable underlying material all contribute to high drainage density. A fine drainage texture is produced by high drainage density, whereas a coarse texture is produced by low drainage density (Strahler, 1964). Drainage Density is calculated by following the formula.

$$Dd = Lu/A \tag{4}$$

Where Lu = Total stream length of all orders, A = Area of basin (km2)

Sometimes, drainage densities are less than 1 km/km2 in very permeable terrain with minimal chance of runoff. Densities over 500 km/km2 are frequently observed on heavily dissected surfaces. Upon detailed examination of the mechanisms generating variation in drainage density, it has been observed that climate, terrain, soil infiltration capacity, vegetation, and geology are among the factors influencing stream density (Pidwirny, 2006). Nag (1998) states that regions with dense vegetation, low relief, and highly resistant or permeable subsurface material are typically associated with low drainage density.

The importance of Dd as a factor influencing how long it takes for water to get to a basin's outlet was noted by Langbein (1947). In contrast to low drainage density basins, which have a delayed hydrologic response, high drainage density basins frequently have a very rapid hydrologic response and a hydrograph with a steep recession (or falling) limb.

Channel Sinuosity (Cs)

A dimensionless parameter called channel sinuosity (Cs) or sinuosity index is created by dividing the length of a stream's real course by the distance between its two endpoints. The channel's midline serves as the measurement for the sinuous length. Sensitive markers of active tectonics include sinuosity indices of rivers in mountainous regions. Rivers rarely travel in a straight line from source to mouth. Changes in slope brought on by the deformation result in adjustments to river channels. Channel sinuosity value 1 corresponds to perfectly straight channel while values close to 1 are characteristically indicators of tectonically active regions. Channels with higher ratios are called meandering channels (Leopold et al., 1964) and are typical of tectonically stable areas.

The channel sinuosity index was used to assess the relative tectonic activity in the Goriganga River basin, proposed by Mueller (1968). For calculating the channel sinuosity index, the below-mentioned formula was used:

$$C_s = \frac{S_l}{V_l} \tag{5}$$

where Cs is the channel sinuosity, Sl is the stream length, and Vl is the valley length.

Valley Floor Width and Height Ratio (Vf)

Valley floor width to height ratio (V_f) was calculated by Bull and McFadden (1977) as a geomorphic measure of active tectonics to distinguish between open, broad valleys in regions of moderate tectonic stability and narrow, deep valleys typical of quickly ascending areas. According to Silva et al. (2003), the Vf illustrates the distinctions between U-shaped, broad-floored valleys with primarily lateral erosion into nearby hill slopes in response to relative base-level stability or tectonic quiescence, and V-shaped valleys occupied by streams incising their bedrocks in response to active uplift. This index, therefore, uses one vertical and one horizontal dimension at a given section across the stream in the erosional system. The V_f index is calculated by the equation:

$$V_f = \frac{2V_{fw}}{(E_{ld} - E_{sc}) + (E_{rd} - E_{sc})} \tag{6}$$

Where, V_{fw} is the width of valley floor and E_{sc} is the elevation of the valley floor. E_{rd} and E_{ld} are the elevations of right and left valley divides respectively (Fig.3).
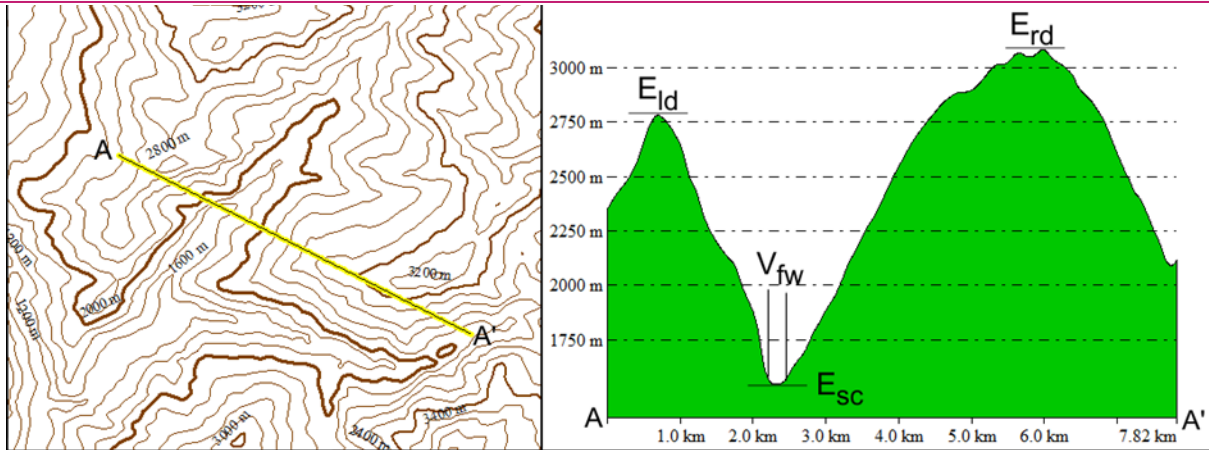
Fig. 3.. *Method of measuring Vf. Profiles along which Eld, Erd and Esc are measured and carefully chosen, such that these are perpendicular to the length of the valleys*

RESULTS AND DISCUSSION

Stream Length Gradient (SL)

Relative tectonic activity is evaluated using the SL index (Keller and Pinter, 2002). When streams and rivers run along strike-slip faults, anomalously low values of SL may also be associated with tectonic activity, even if high values of SL suggest recent tectonic activity (Keller and Pinter, 2002; Moussi et. al., 2018). Standardized average SL values for each of the 32 sub-basin streams were calculated for this study. SL values ranged from 1 to 5 reaches on average, depending on the stream's length. The reach length might be anything between 500 m and 5 km long.

Values of Stream Length Gradient Index (SL) for the Goriganga range from 18 to 4737, indicating that these values corrugate tectonic variation within the basin. Three classes—Class 1 (18 to 690), Class 2 (691 to 2750), and Class 3 (2751 to 4737)—were assigned to these values. Fig. 4 displays the outcomes of the Stream Length Gradient (SL) classification. It is evident that, in comparison to the other basin areas, the south and east-central sections of the Goriganga's left bank are more active tectonically.

The strong tectonic turbulence produces low values of the stream length gradient along the trunk stream of the Goriganga river basin, comparably to the central-eastern parts of the basin. The central-eastern region of the basin falls in between the Vaikrita thrust and the Trans-Himadri Fault. It indicates active neotectonic control over the region(Fig. 1).

Hypsometric Integral (HI)

Hypsometric Integral (HI) was computed for the 32 sub-basins of the Goriganga watershed. The values range from 0.26 to 0.57. Further, these values are classified into three classes: Class 1 (< 0.30), indicating denuded topography, low rates of uplift and tectonic activity; Class 2 (0.30 to 0.45) indicating more youthful land-
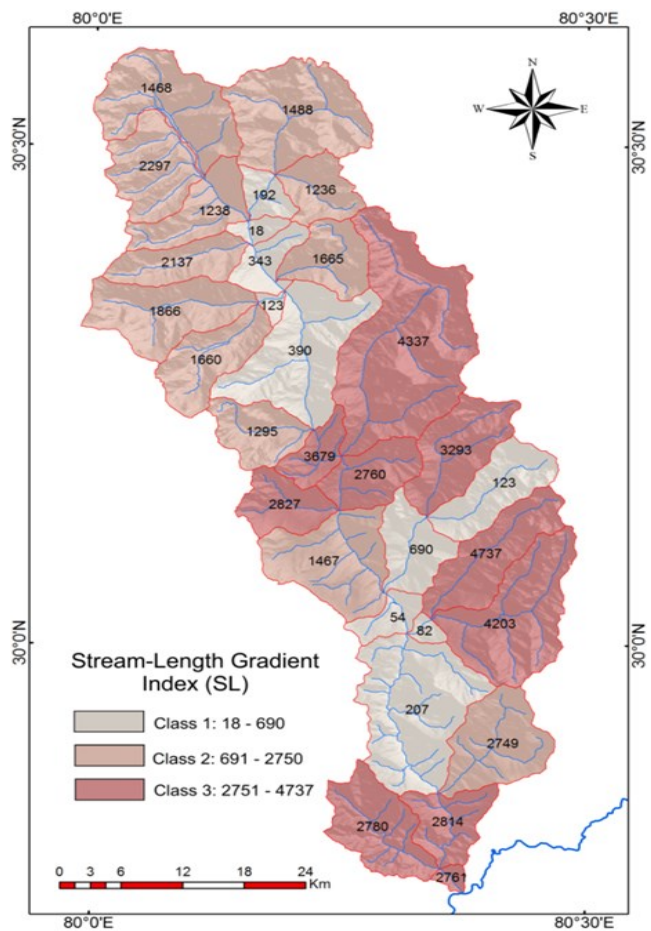

Fig. 4. *Showing the spatial variability of Stream Length Gradient within Goriganga*

scape, moderate rate of uplift and Class 3 (> 0.45), indicating a high rate of uplift and most youthful topography comparatively.

faults and lineaments (Askote Clippe, Anticlinal and Synclinal axis) (Fig. 6). Remarkably, the Kali River, of which the Goriganga is a significant right bank tributary, flows over a linear stretch of rapid erosion, encouraging the construction of an anticlinal structure with its axis transverse to the Himalayan main trend (Montgomery
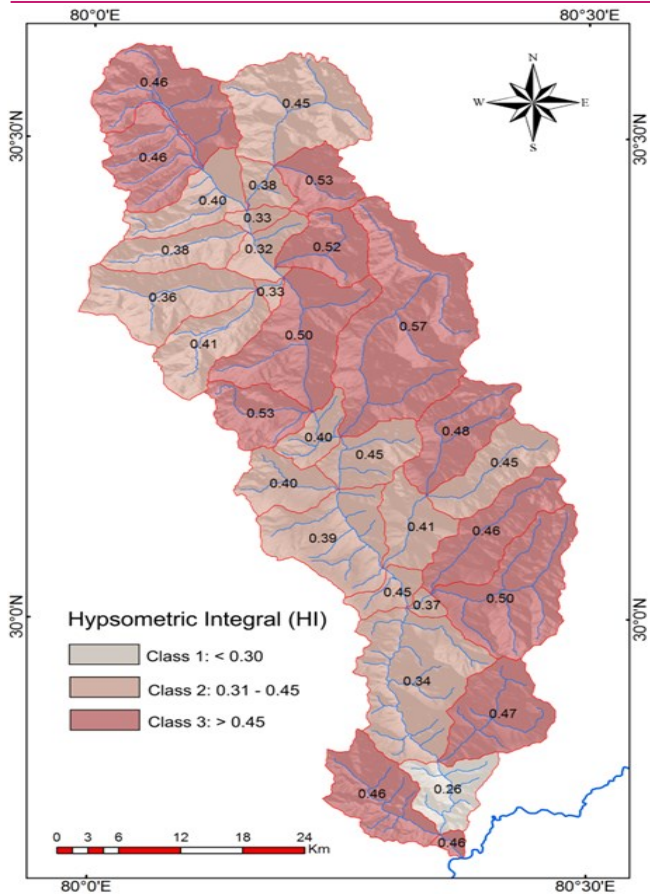
Fig. 5. *Showing geographical variation of Hypsometric Integral results derived from ASTER data*
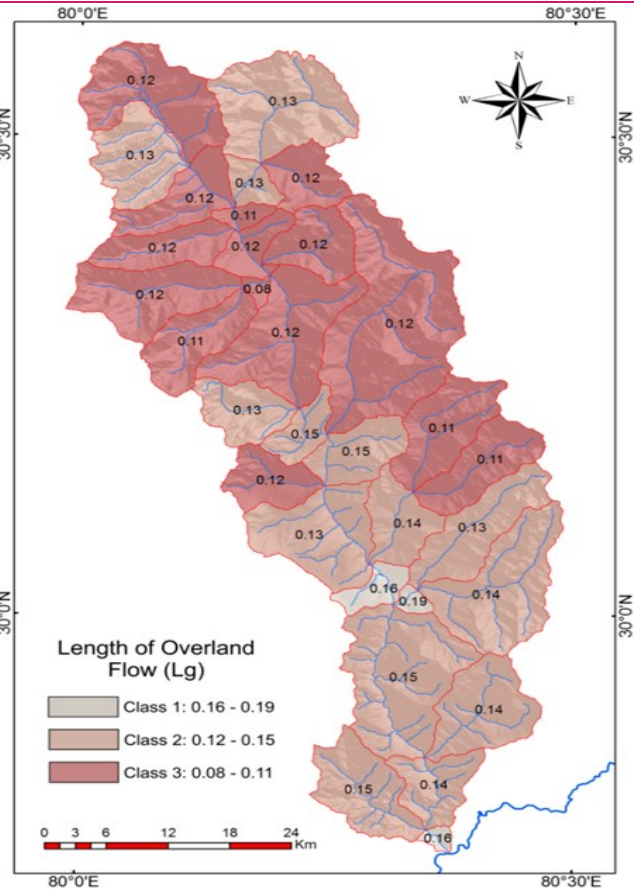

Fig. 7. *Depicting spatial variation of Length of Overland Flow within the basin*
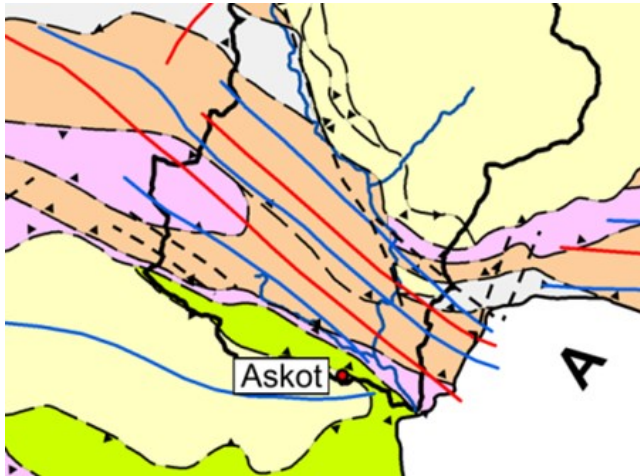

Fig. 6. *Showing active control of tectonic Over Rauntis Gad sub-basin*

Fig. 8. *Faults scarp along the Bashura Dhar in the Kholiagaon*

and Stolar, 2008). High levels of HI along the eastern bank of the Goriganga support the idea that trans-Himalayan River courses predating the Himalayan orogeny are associated with regions of relatively high rates of active tectonics in the Himalaya perpendicular to the main grain of Trans Himadri Fault (THF) on the both east and west banks of Goriganga. Southern region which is experiencing moderate tectonic activity as per the results of Length of Overland Flow (Lg) indicat-

ed moderate tectonic activity. However, this region is also transecting with active faults and lineaments. However, in this central southern region, fluvial processes were dominant to regulate erosion and cannot be neglected.

Two sub-basins expressed the highest values of Lg, indicating lesser tectonic activity than the rest. It means these are dominated by erosional processes rather than tectonic activity due to their proximity to the trunk
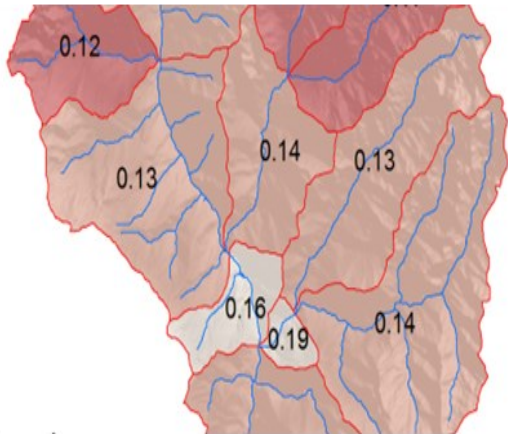
Fig. 9. *Showing highest values of Lg, correspond to high overland flow, correspondingly low tectonic activity*

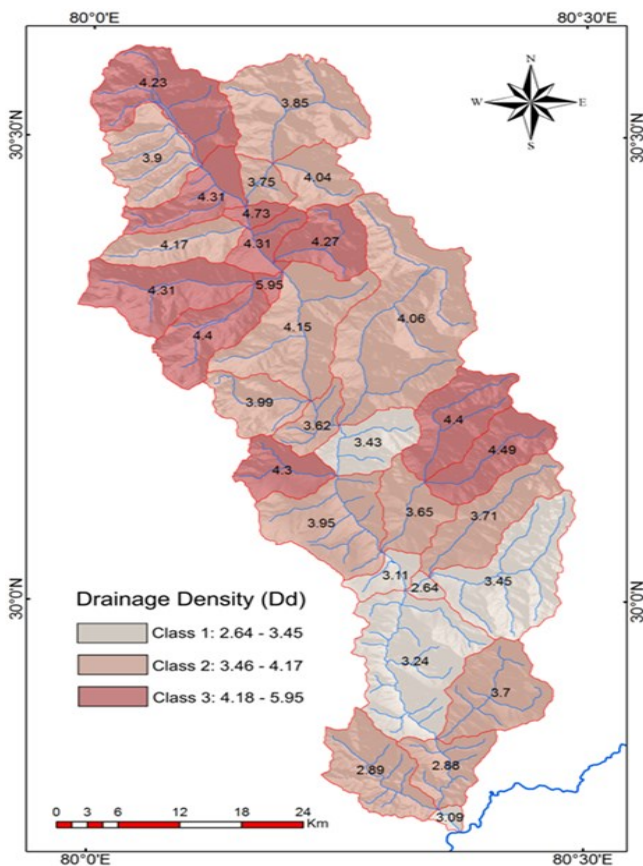**Fig. 11.** *Red Fault line shows Trans Himadri Fault, followed by Goriganga*

Fig. 10. *expresses Spatial Variability in Drainage density in the Goriganga River Basin*
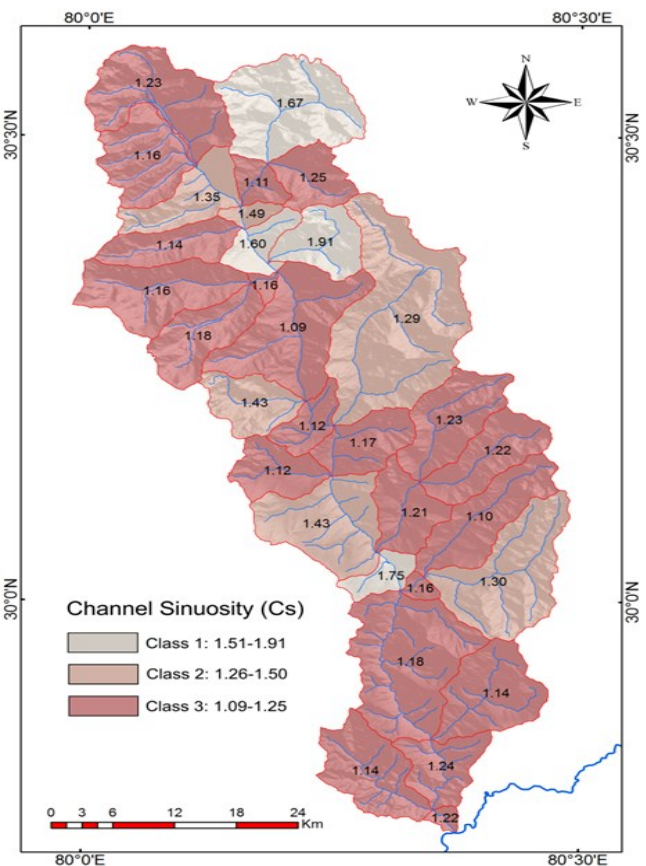

Fig. 12. *Showing values of Channel Sinuosity, indicating tectonic activity within the basin*

stream and their size.

It can be readily appreciated that the sub-basins of the northern half of the Goriganga are somewhat more tectonically active than those of the southern half, as indicated by the Lg index (Fig. 9).

Drainage Density (Dd)

Results of Drainage Density (Dd) were calculated and classified into three classes: Class1 (2.64 to 3.45), Class 2 (3.46 to 4.17) and Class 3 (4.18 to 5.95), as shown in Fig. 10.

Since the northwest is composed of Tethys deposits and Vaikrita formations, it has a relatively high drainage density and surface permeability. High drainage densities are also associated with a range of tectonic consequences. The southern region has moderate drainage density values corresponding to active faults and lineaments leading to a relatively high infiltration rate (Khairuddin et. al., 2017).

The southern region has moderate drainage density values corresponding to active faults and lineaments, leading to a relatively high infiltration rate.
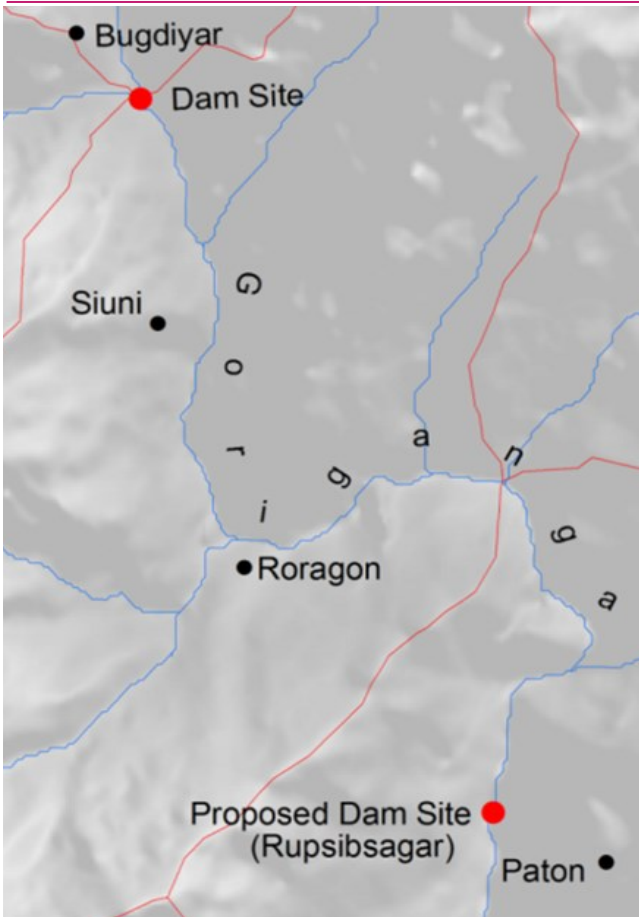
Fig. 13. *Showing proposed Dam Sites and Bogdiyar Meander. It comes in very high tectonically active region*

Fig. 14. *Valley Floor Width to Height Ratios (Vf) of the sub-basins of the Goriganga.*

Channel Sinuosity Index (Cs)

In order to differentiate the relative tectonic activity of the sub-basins, the Cs values were classified into three classes: Class 1 (1.09 to 1.25), Class 2 (1.26 to 1.50), and Class 3 (1.51 to 1.91) as illustrated in Fig. 9. The sinuosity indices for the 32 sub-basins of the Goriganga range from 1.09 to 1.91.

A few stream reaches show unusually high Cs values (Fig. 12). These anomalies may have produced from offsets of the reaches caused by displacements along transverse faults or shear zones rather than from the typical uplift/erosion processes. These have not been taken into account when classifying the sub-basins according to relative active tectonics. A river's high sinuosity in level areas can be explained by the extremely low angles of the ground slope, but in mountainous areas, tectonic-structural features can greatly enhance a channel's sinuosity.

Schumm (1963) and Gaurani et al., (2023) identified 5 categories of channel sinuosity viz., straight course when channel sinuosity is 1.0, transitional course, regular course, irregular course and tortuous course (when channel sinuosity is more than 20). Values of channel sinuosity of 6th and 7th order streams in the Goriganga basin range from 1.03 to 1.91.
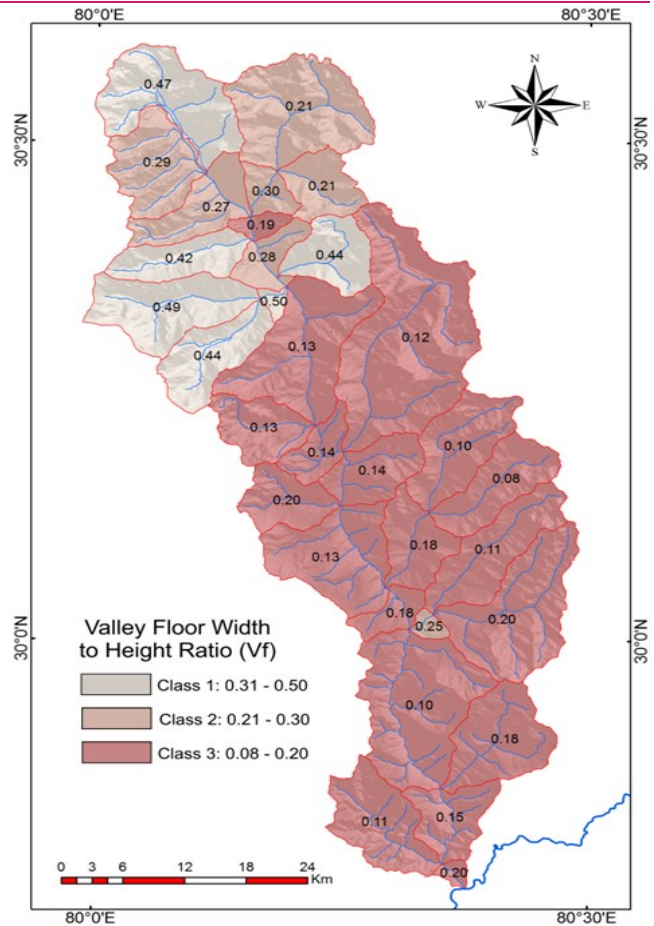
Valley Floor Width and Height Ratio (Vf)

The number of measurements and the spacing between them varied with the size of the sub-basin. The values of Vf, which ranged from 0.08 to 0.50 for the whole Goriganga basin, were calculated for each sub-basin based on the mean of several readings in each sub-basin. Three categories were assigned to Vf: Class 1 (0.08 to 0.19), Class 2 (0.20 to 0.30), and Class 3 (0.31 to 0.50).

While sub-basins classified as Class 3 are filled by rivers running in small, steep-sided valleys, indicating a high degree of tectonic activity, sub-basins classified as Class 1 have large U-shaped valleys, indicating topographic maturity and, consequently, less tectonic activity. All of the Goriganga basin's sub-basins have Vf indices smaller than 1.0, as seen in Fig. 5, which suggests a high level of tectonic activity overall. However, on the basis of the Vf index, the central and southern parts of the basin have a somewhat higher rate of uplift than the northern part.

Conclusion

It is concluded that there is strong neotectonic control over the evolution of the Goriganga River Basin due to

known and unknown faults, lineaments, and thrusts. Additionally, meandering streams, parallel tributaries, tilted sub-basins, extended valleys, and active faults are manifestations of the effects of tectonic struggle. As it stands, the Rauntis and Baram Faults continuously alter the valley.

The tectonic activity that predominated around the Trans Himadri Fault, Main Central Thrust, and Munisiari Thrust significantly altered the drainage network of the Goriganga river basin, as seen by the Stream Length Gradient (SL) and Channel Sinuosity, such as the Bogdyar meander. However, due to glacial erosion, which shapes their valleys into a U shape, only a few sub-watersheds are exhibiting correspondingly modest tectonic activity.

The Goriganga River basin is determined to be tectonically active. Additionally, the forms and processes that are causing the active deformation are greatly impacted by the ongoing tectonic activity. The strength of these processes is great enough to cause rivers to diverge from their original paths (Bogdyar Meander, almost right angle turn at Trans Himadri Fault), the construction of linear and serrate ridges, fault scarps, etc., close to established faults and thrusts, among other things.

Conflict of interest

The authors declare that they have no conflict of interest.

REFERENCES

1. Bookhagen, B. & Burbank, D.W. (2006). Topography relief and TRMM derived rainfall variations along the Himalayas. *Geophysical Research Letters*, 33(8), 1–5. https://doi.org/10.1029/2006GL026037

2. Bull W. & L.D. McFadden. (1977). Tectonic Geomorphology North and South of the Garlock fault. California, *Journal of Geomorphology*, 1, 15-32.

3. Burbank, D.W. & Anderson, R.S. (2011). *Tectonic Geomorphology*, 2nd Edition, Malden USA, Blackwell Publishing, 274 pp.

4. Dowling, T.I., Richardson, D.P., O'Sullivan, A., Summerell, G.K. & Walker, J. (1998). Applications of the hypsometric integral and other terrain based metrices as indicators of catchment health: A preliminary analysis. *CSIRO Land and Water, (Canberra). Technical Report* 20/98, 49 p.

5. Farooq, S. & Khan, M.N. (2017). Basin Asymmetry Index is an Indicator of Active Tectonics in Goriganga River Basin, Eastern Kumaon Himalaya, *IJAEES*, 8(1).

6. Farooq, S. Khan, M.N. & Sharma, I. (2015). Assessment of Active Tectonics in Eastern Kumaon Himalaya on the Basis of Morphometric Parameters of Goriganga River Basin, *IJAEES*, 3(1), 14-21.

7. Ghosh, S. (2011). Quantitative and Spatial Analysis of Fluvial Erosion in Relation to Morphometric Attributes of Sarujharna Basin, east Singhbhum, Jharkhand. *International Journal of Geomatics and Geosciences*, 2(1), 71-90.

8. Goldsworthy, M. & Jackson, J. (2000). Active normal fault evolution in Greece revealed by geomorphology and drainage patterns. *Journal of the Geological Society*, 157 (5), 967–981.

9. Hack, J.T. (1973). Stream profile analysis and stream-gradient index, *J. Res. U.S. Geol. Surv.*, 1,421-429.

10. Horton, R.E. (1932). Drainage basin characteristics, *Trans. Amer. Geophys. Union*, 13, 350-361.

11. Horton, R.E. (1945). Erosional development of streams and their drainage basins: Hydrophysical approach to quantitative morphology. *Geological Society of America Bulletin*, 56, 275-370. http://www.geog.leeds.ac.uk/people/a.turner/research/interests/geomorphometrics/Developing%20and%20Using%20Geomorphometrics0.3.1.doc.

12. Joshi, L.M. & Kotlia, B.S. (2015). Neotectonically triggered instability around the palaeolake regime in Central Kumaun Himalaya, India. *Quaternary International*, 371, 219–231.

13. Gaurani, K. Kothyari, G.C. & Kotlia, B.S. (2023). Morphotectonic assessment of the Gaula river basin, Kumaun lesser Himalaya, Uttarakhand, *Quaternary Science Advances*, 12, 100-115. https://doi.org/10.1016/j.qsa.2023.100115.

14. Keller, E.A. and Pinter, N. (2002). Active Tectonics: Earthquakes, Uplift and Landforms (2nd Edition). Prentice Hall, New Jersey. 362 pp. ISBN: 0130882305.

15. Khan, M.N., Khudoyarova S.S., Juraev J., Mamajanov R.I., (2023). Field-based Tectonic Assessment and Spatial Correlation with Land Use and Land Cover in the Goriganga River Basin, *Bulletin of Pure and Applied Sciences-Geology*, 42 (1), 32-45. https://doi.org/10.48165/bpas.2023.42F.1.4

16. Khaerudin, D. N., Suharyanto, A., & Harisuseno, D. (2017). Infiltration Rate for Rainfall and Runoff Process with Bulk Density Soil and Slope Variation in Laboratory Experiment. *Nature Environment & Pollution Technology*, 16(1).

17. Kothyari, G. C., Kandregula, R. S., & Luirei, K. (2017). Morphotectonic records of neotectonic activity in the vicinity of North Almora Thrust Zone Central Kumaun Himalaya. *Geomorphology*, 285, 272–286.

18. Kothyari, G.C. & Pant, P. D. (2008). Evidences of active deformation in the northwestern part of Almora in Kumaun Lesser Himalaya: A geomorphic perspective. *Geological Society of India*, 7.

19. Kothyari, G.C., Shukla, A.D. & Juyal, N. (2017). Reconstruction of late Quaternary climate and seismicity using fluvial landforms in Pindar River Valley Central Himalaya, Uttarakhand, India. *Quaternary International*, 443, 248–264. https://doi.org/10.1016/jquaint201606001

20. Kothyari, Girish C., Kotlia, Bahadur S., Talukdar, Riyanka, Pant, Charu C., Joshi, M. (2020). Evidences of neotectonic activity along Goriganga River, Higher Central Kumaun Himalaya, India, *Geological Journal*, 55 (9), 0072- 1050.

21. Kotlia, B. S., Sanwal, J., Phartiyal, B., Joshi, L. M., Trivedi, A. & Sharma, C. (2010). Late Quaternary climatic changes in the eastern Kumaun Himalaya India as deduced from multi-proxy studies. *Quaternary International*, 213(1–2), 44–55.

22. Kotlia, B.S. & Joshi, L. M. (2013). Neotectonic and climatic impressions in the zone of Trans Himadri Fault (THF) Kumaun Tethys Himalaya India: A case study from palae-

olake deposits. *Zeitschrift für Geomorphologie*, 57(3), 289 –303.

23. Kotlia, B.S., & Rawat, K.S. (2004). Soft sediment deformation structures in the Garbyang palaeolake: Evidence for the past shaking events in the Kumaun Tethys Himalaya. *Current Science*, 87(3), 377–379.

24. Langbein, W.B. (1947). Topographic characteristics of drainage basins. *U.S. Geol. Surv. Water-Supply Paper* 986 (C), 157-159.

25. Larson, K.P & Godin, L. (2009). Kinematics of the Greater Himalayan sequence, Dhaulagiri Himal: Implications for the structural framework of central Nepal. *Journal of the Geological Society*, 166(1), 25-43.

26. Leopold, L.B., Wolman, M.G. and Miller, J.P. (1964). Fluvial processes in geomorphology, Dover Publications, New York. 531 pp.

27. Mahmood, S.A. and Gloaguen, R. (2012). Appraisal of active tectonics in Hindu Kush: Insights from DEM derived geomorphic indices and drainage analysis. *Geoscience Frontiers*, 3(4), 407-428.

28. Mohammad S. (2014). Morphometric Analysis of Umred Watershed of Wainganga River Basin: Using Cartosat DEM and GIS Techniques, *Excellence International Journal of Education and Research*, 2(9), 255-269. ISSN: 2322-0147.

29. Montgomery, D.R. & Stolar, D.B. (2006). Reconsidering Himalayan river anticlines, *Geomorphology*, 82, 4-15.

30. Moussi, A., Rebaï, N., Chaieb, A. & Saâdi, A. (2018). GIS-based analysis of the Stream Length-Gradient Index for evaluating effects of active tectonics: a case study of Enfidha (North-East of Tunisia). *Arab J Geosci* 11, 123. https://doi.org/10.1007/s12517-018-3466-x

31. Mueller, J.E. (1968). An introduction to the hydraulic and topographic sinuosity indices. *Annals Association of American Geographers*, 58(2), 371-385.

32. Nag, S.K. (1998). Morphometric analysis using remote sensing techniques in the Chaka sub-basin Purulia district, West Bengal, *J. Indian Soc. Remote Sensing*, 26, 69-76. DOI: 10.1007/BF03007341.

33. Omar M.A. Radaideh, Jon, M. (2019). Tectonics controls on fluvial landscapes and drainage development in the westernmost part of Switzerland: Insights from DEM derived geomorphic indices, *Tectonophysics* 768.

34. Pathak, V., Pant, C.C., Darmwal, G.S. (2013). Geomorphological and seismological investigations in a part of western Kumaun Himalaya Uttarakhand, India. *Geomorphology*, 193, 81–90.

35. Pazzaglia, F.J. (2013). Fluvial terraces chapter 923. Department of Earth and Environmental Sciences, Lehigh University: Elsevier

36. PérezPena, J.V., Azor, A., Azanón, J. M. & Keller, E. A. (2010). Active tectonics in the Sierra Nevada (Betic Cordillera Se Spain): Insights from geomorphic indexes and drainage pattern analysis. *Geomorphology*, 119, 74–87.

37. Pidwirny, M. (2006). "Stream Morphometry". Fundamentals of Physical Geography, 2nd Edition [Online]. Available online: http://www.physicalgeography.net/fundamentals/10

ab.html. Accessed: 26 June 2012.

38. Schumm, S.A. (1963). Sinuosity of alluvial rivers on the Great Plains. *Geological Society of America Bulletin*, 74 (9), 1089-1100.

39. Schumm, S.A., Dumont, J.F. & Holbrook, J.M. (2002). Active tectonics and alluvial rivers: Cambridge University Press, Cambridge. 276 pp. ISBN: 0 521 66110 2.

40. Strahler, A.N. (1964). *Quantitative geomorphology of drainage basins and channel networks*, Section 4 Part II. In: Chow, V. T. (Ed.), *Handbook of Applied Hydrology*. New York, McGraw Hill Book Company. 39-76.

41. Taib, H., Hadji, R., Hamed, Y. (2023). Exploring neotectonic activity in a semiarid basin: a case study of the Ain Zerga watershed. *Journal Umm Al-Qura Univ. Applied. Science*. DOI: https://doi.org/10.1007/s43994-023-00072-3

42. Tricart, J. (1974). *Structural geomorphology*. London: Longman. p. 305

43. Turner, A. (2006). Geomorphometrics: Ideas for Generation and Use. CCG Working Paper, Version 0.3.1. Centre for Computational Geography, University of Leeds, UK.

44. Twidale, C. R. (1971). Structural landforms: Landforms associated with granitic rocks faults and folded strata (pp. 97–138). Canberra: ACT: Australian National University Press.

45. Valdiya, K. S. (1980). *Geology of Kumaun lesser Himalaya* (Vol. 280). Wadia Institute of Himalayan Geology. Rajpur Road Dehradun: Himachal times press.

46. Valdiya, K.S. (1976). Himalayan transverse faults and folds and their parallelism with subsurface structures of North Indian plains. *Tectonophysics*, 32(3/4), 353–386.

47. Valdiya, K.S. (1992). Active Himalayan Frontal Fault Main Boundary Thrust and Ramgarh Thrust in Southern Kumaun. *Journal of Geological Society of India*, 40(6), 509–528.

48. Valdiya, K.S. (1993). Uplift and geomorphic rejuvenation of the Himalaya in the Quaternary period. *Current Science*, 64(11/12), 873–885.

49. Valdiya, K.S. (1993). Uplift and geomorphic rejuvenation of the Himalaya in the Quaternary period. *Current Science*, 64(11/12), 873–885.

50. Valdiya, K.S. (2001). Reactivation of terrane-defining boundary thrusts in central sector of the Himalaya: Implications. *Current Science*, 81(11), 1418–1431.

51. Valdiya, K.S. (2010). *The Making of India: Geodynamic Evolution*. New Delhi, Macmillan Publishers India Ltd. 816 pp. ISBN: 0230-32833-4.

52. Wallace, R.E. (1990). The San Andreas Fault System, California: US Geological Survey Professional Paper 1515, United States Government Printing Office, Washington, DC, 283 pp.

53. Willett, S.D., Hovius, N., Brandon, M.T., and Fisher, D.M. (2006). Introduction, in Willett, S.D., Hovius, N., Brandon, M.T., and Fisher, D.M. (Eds). *Tectonics, Climate, and Landscape Evolution. Geological Society of America Special Paper 398*, Penrose Conference Series, vii-xi. DOI: 10.1130/2006.2398(00).